Improving Spatial and Temporal Resolution of Electrical Impedance Tomogram (EIT) by Partial Imaging with Limited Measurements (PILM)

Qiang Wang*, Bishal Karki, Yousef Faraj and Mi Wang

Institute of Particle Science & Engineering, University of Leeds, LS2 9JT, UK.
pmqw@leeds.ac.uk

ABSTRACT

In the past few decades, EIT systems have been successfully applied to many different industries, such as petroleum, chemical and energy. The performance of existing EIT-based multi-phase flow metering is, however, still challenging, due to incapability of current EIT systems for providing both qualitative spatial and temporal resolution at the same time. On the other hand, one important characateristics of multi-phase upward pipeline flow is that the flow regimes can be assumed in radial symmetrical over the cross-section of the pipe under investigation, which means the central area of a tomogram can be utilised to approximate the whole tomogram when calculating multi-phase flow characteristics, e.g. concentration and velocity. This paper proposes a novel approach to achieve reasonable spatial and temporal resolution for multi-phase flow metering by partially imaging multi-phase flow with limited measurements by means of reducing the number of injection and measurement pairs during gauging process, without changing the original configuration of 16-electrode based EIT system, and back projection based image reconstruction. Experiments were conducted in terms of visualising static objects in a phantom and metering gas-water 2-phase upward vertical flow. The results demostrated that the proposed approach generates comparable tomograms to the ones obtained by conventional 16-electrode EIT system, and offers a great temporal resolution, which is suitable for velocity extraction using conventional cross-correlation method, which further improves the performance of EIT-based multi-phase flow metering.

Keywords Electrical Impedance Tomography, Partial Imaging with Limited Measurements, Multi-phase Flow Metering

1 INTRODUCTION

Electrical impedance tomography (EIT) has been used to obtain both qualitative and quantitative data from multi-phase flow systems. It is well known that distinct features of EIT are its relatively low spatial resolution and high temporal resolution. In order to obtain accurate measurements from EIT based multi-phase flow metering, it is necessary to maintain optimum level of spatial and temporal resolution. When measuring velocity distribution of disperse phase in multiphase flow using cross correlation method, discrimination error κ can be used to assess the accuracy of EIT which can be expressed as(BECK and PLASKOWSKI, 1987):

$$\kappa = \frac{\delta}{2\tau} \quad (1)$$

Where τ is the time required for a flow passing the dual-plane sensor, and δ is the flow velocity.

If the distance between the two sensing planes of a dual-plane sensor is 0.05m and flow velocity is 10m/s then τ = 0.005s. For a discriminatory precision of 5%, i.e. δ = 0.0005s, the speed of 2000 dual-frames per second is required. Therefore higher speed of EIT is necessary in order to achieve higher accuracy. Reducing the number of electrodes will increase the speed but the temporal resolution will suffer making it unsuitable for flow visualisation. The motivation behind the present work is to enhance the temporal resolution without compromising the spatial resolution.

Resolution of EIT is largely dependent on the data collection strategy employed. Adjacent sensing strategy, reported by Baber and Brown in 1984 (BARBER and BROWN, 1984), applies current through two adjacent electrodes and the voltage difference is measured between all other successive pairs of adjacent electrodes. The number of independent measurement, excluding the measurement from current injecting electrodes, is governed by N*(N-3)/2, where N is the number of electrodes. Since most of the current travels around the periphery in this strategy, the current density is relatively low at the centre. Another common method is the so-called opposite strategy (HUA, et al., 1987), where current is applied to the electrodes which are diametrically opposite to each other and the voltages are measured at all electrodes except the current injecting electrodes. Current flows largely through the centre rather than at the boundary of the vessel, and therefore sensitivity distribution is higher at centre. For N electrodes, the number of independent measurements offered by opposite strategy is given by N/4*(3N/2 – 1). Due to less number of independent measurements compared to adjacent strategy, the image solution is relatively poorer. In diagonal strategy (BRECKON and PIDCOCK, 1987), current is injected between electrodes separated by large distance. For the configuration of 16 electrodes, this strategy requires 182 data points, 104 of which are independent. This strategy claims higher sensitivity compared to adjacent method, and also offers better image quality as it is less sensitive to measurement error. Since the choice of sensing strategy depends on the region of interest, as the sensitivity varies for each strategy in different regions of the domain (DA TORRE PINHEIRO, 1994), adjacent strategy, therefore, is chosen for our study due to its advantages, e.g. higher number of independent measurements, and relatively simple and undemanding implementation of hardware and software.

Efforts have been made to improve spatial and temporal resolution of EIT systems by means of Asymmetrical Sensing and Imaging (ASI) strategy on scale and vector tomograms (WANG et al., 2014). The study investigated the possibility of retaining the speed offered by conventional 8-electrode EIT while achieving good-quality tomograms comparable to the ones by conventional 16-electrode EIT, by reallocating 8 electrodes to 16-electrode configuration of conventional EIT systems. Since the hardware configuration had to be changed, conventional one-step reconstruction algorithms, e.g. sensitivity theorem-based back-project (KOTRE, 1994a), was no longer applicable, and therefore sensitivity theorem-based conjugate-gradient iterative method (SCG) (WANG, 2002) was utilised to reconstruct tomograms. The results, however, demonstrated that ASI was unable to produce promising images comparable to the ones by conventional 16-electrode configuration, and further concentration and velocity profiles of gas-water 2-phase upward flow in vertical pipeline, although the results was better than that generated by conventional 8-electrode EIT. As a result, simply reducing the number of electrodes is incapable of fulfilling our primary objectives, and hence alternatives should be sought.

2 METHODS

Flow characteristics of multiphase flow such as disperse phase concentration and velocity distributions can be assumed as either radial symmetrical in vertical pipeline or central-vertical plane symmetrical in horizontal pipeline. The necessary and minimum imaging area, which can represent the major features of pipeline flows when both cases are combined, is the row of pixels along the central-vertical plane, as indicated in Figure 1 (a).

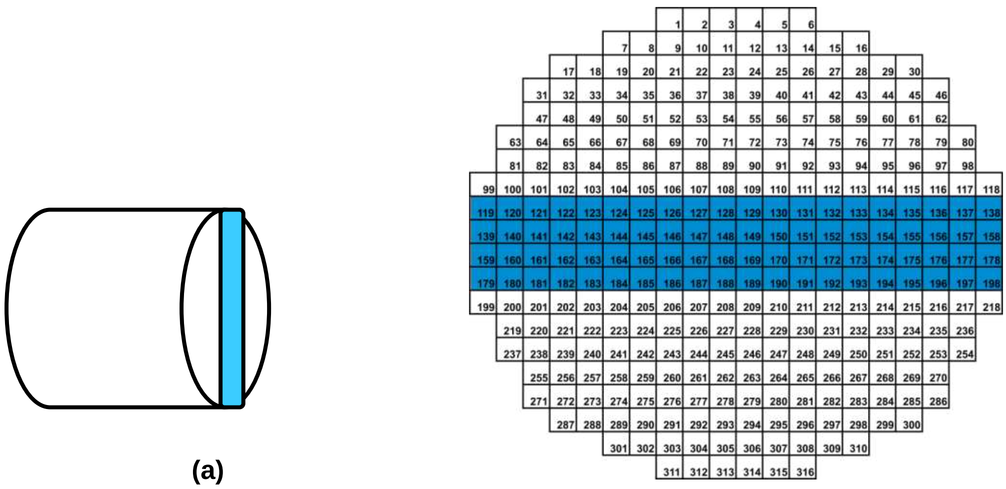

(a)

(b)

Figure 1: (a) symmetrical feature of pipeline flows, (b) arrangement of 316 tomogram elements by 20*20 grid (INDUSTRIAL TOMOGRAPHY SYSTEMS2009)

Therefore, targeting only the central one or few rows of the full tomogram as shown in Figure 1 (b) will result in lesser number of measurements thereby increasing the speed while maintaining the spatial resolution to a comparable level. A new sensing strategy, based on 16 electrodes EIT, called Partial Imaging with Limited Measurements (PILM) was developed in order to achieve similar performance to conventional EIT using limited measurements. Figure 2 compares sensitivity maps by conventional adjacent strategy and PILM. Since PILM targets few central rows of conventional tomograms, Figure 2 (b) masks the unconcerned area of full sensitivity map. Comparing Figure 2 (b) and 2 (c), it can be seen that PILM's sensitivity map is very close to conventional one, and therefore is expected to produce comparable measurements during application.

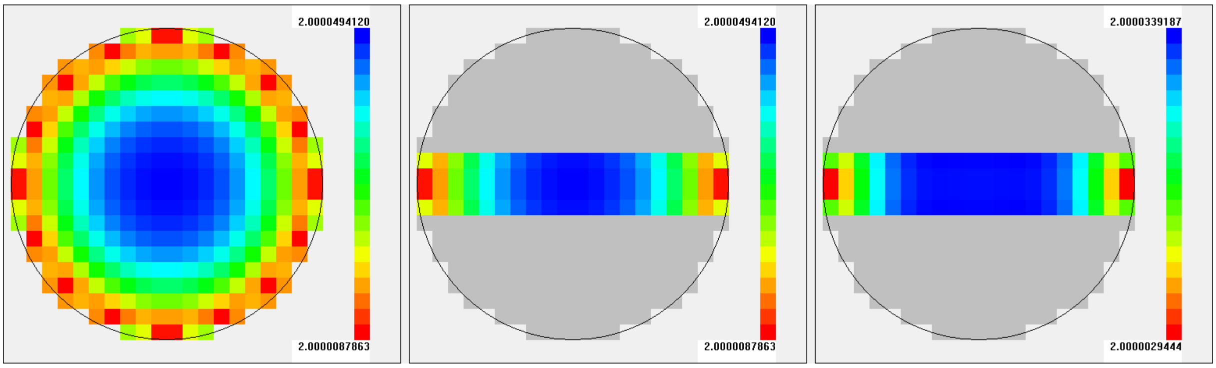

(a) (b) (c)

Figure 2: Sensitivity map: (a) full sensitivity map for adjacent measurement, (b) central axial sensitivity map for adjacent measurement, and (c) sensitivity map for PILM

2.1. PILM sensing strategy

The sensing strategy of PILM consists of three groups of excitation and measurement electrode pairs arranged in rotary, parallel and complimentary positions as shown in Figure 3 (a), (b) and (c) respectively. Each projection is carried out by applying current to a pair of electrodes and measuring voltage from other pair of electrodes corresponding to the electrode pairs adjacent to the terminals of each rectangular bar in Figure 3. Based on the reciprocity theorem, no mutual projection (excitation and measurement) is required. Therefore a total of 20 measurements i.e. 8 for rotary, 6 for parallel and 6 for complimentary position are required to focus the sensitivity in the central region as illustrated in Figure 3 (d) and (e). Since 256 measurements are made for a single scan by a 16 electrode EIT system, PILM reduces the measurements to a mere 20 per scan using the same system resulting in dramatic increase in speed.

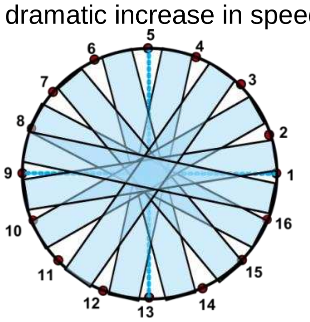

(a)

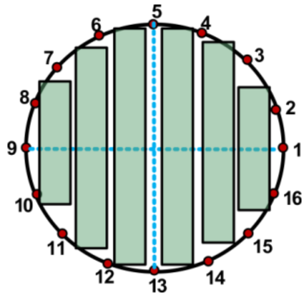

(b)

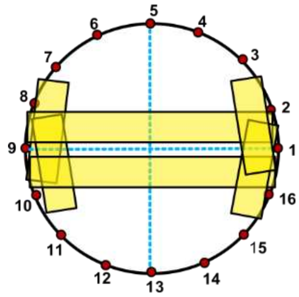

(c)

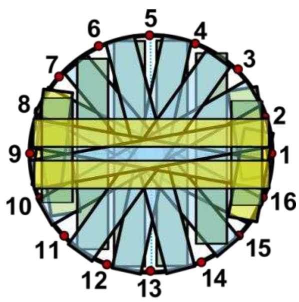

(d)

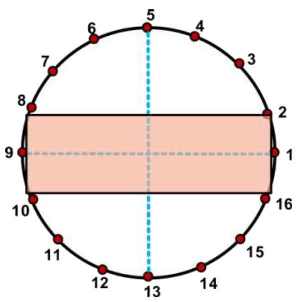

(e)

Figure 3: PILM sensing strategy, (a) Rotary band, (b) Parallel band and (c) Complimentary band, (d) Overall projections, (e) Region of high sensitivity

Along with the reduction in number of measurements, PILM also results in reduction of computation required for conductivity reconstruction.

One of the widely applied one-step reconstruction method is sensitivity theorem based back-projection(KOTRE, 1994b, WANG, 2002) which is governed by equation 2:

$$[\Delta\boldsymbol{\sigma}]_{N\times 1} = 1 - [S]_{N\times M} \cdot [\Delta\boldsymbol{V}]_{M\times 1} \qquad (2)$$

where, $[S]_{N\times M}$ is pre-defined sensitivity matrix,
$[\Delta\boldsymbol{\sigma}]_{N\times 1}$ is the relative change of mixture conductivity, and
$[\Delta\boldsymbol{V}]_{M\times 1}$ is the relative change of measured voltages for N = 1, 2, ……, n and M = 1, 2, ……, m.

Equation 2 can be used to produce a full conductivity tomogram, for example, of 316 elements as shown in Figure 2 (b) from a full set of measured voltage data using conventional sensing strategy. The limited measurements required for PILM can be derived from full set of measured voltages as

$$[\Delta\boldsymbol{V}']_{M\times 1} = [T]_{M\times M} \cdot [\Delta\boldsymbol{V}]_{M\times 1} \qquad (3)$$

where, $[T]_{M\times M}$ is a diagonal matrix, whose diagonal elements are either 1 or 0.
It transforms the full measurement voltage vector to vector $[\Delta\boldsymbol{V}']_{M\times 1}$ such that it has non-zero elements which correspond to the measurements required for PILM.
As mentioned earlier, PILM focuses on the central vertical region of pipeline flow. Hence the region of interest is limited to the central 4 rows of the full tomogram with 316 elements as illustrated in Figure 3 (b). The sensitivity matrix can be modified to set all of its elements to zero except the ones indexed from 119 to 198 which correspond to the elements in the central region of the grid as highlighted in Figure 3 (b).
Therefore, for PILM, equation 2 becomes,

$$[\Delta\boldsymbol{\sigma}']_{N\times 1} = 1 - [S']_{N\times M} \cdot [\Delta\boldsymbol{V}']_{M\times 1} = 1 - [S']_{N\times M} \cdot [T]_{M\times M} \cdot [\Delta\boldsymbol{V}]_{M\times 1}$$

$$= 1 - \begin{bmatrix} 0 & \cdots & 0 \\ \vdots & \vdots & \vdots \\ 0 & \cdots & 0 \\ S_{119,1} & \cdots & S_{119,m} \\ \vdots & \vdots & \vdots \\ S_{198,1} & \cdots & S_{198,m} \\ 0 & \cdots & 0 \\ \vdots & \cdots & \vdots \\ 0 & \cdots & 0 \end{bmatrix}_{N\times M} \cdot \begin{bmatrix} t_1 & 0 & 0 \\ 0 & \ddots & 0 \\ 0 & 0 & t_m \end{bmatrix}_{M\times M} \cdot [\Delta\boldsymbol{V}]_{M\times 1}$$

$$[\Delta\boldsymbol{\sigma}']_{N\times 1} = 1 - \begin{bmatrix} 0 & \cdots & 0 \\ \vdots & \vdots & \vdots \\ 0 & \cdots & 0 \\ t_1 S_{119,1} & \cdots & t_m S_{119,m} \\ \vdots & \vdots & \vdots \\ t_1 S_{198,1} & \cdots & t_m S_{198,m} \\ 0 & \cdots & 0 \\ \vdots & \cdots & \vdots \\ 0 & \cdots & 0 \end{bmatrix}_{N\times M} \cdot [\Delta\boldsymbol{V}]_{M\times 1} \qquad (4)$$

Since t_i is either 1 or 0, some columns of the first matrix in Equation 4 are entirely zeros. $[\Delta\boldsymbol{V}]_{M\times 1}$ can be interchanged with $[\Delta\boldsymbol{V}']_{M\times 1}$ in Equation 4 as the result of matrix multiplication is the same irrespective of $[\Delta\boldsymbol{V}]_{M\times 1}$ or $[\Delta\boldsymbol{V}']_{M\times 1}$ due to the presence of zero elements in the sensitivity matrix. By removing the zero filled columns and rows, in both the matrices, their dimensions can be decreased that will significantly reduce the time and resources required for the computation of matrix multiplication, and further relative conductivity. Taking the example given by the article, with 20 independent measurements and the 80 elements as demonstrated in Figure 2, the computation is reduced from [316, 104]*[104] to [80, 20]*[20]. This computational improvement of more than one order promises to significantly enhance the overall performance of proposed method.

2.2. Experimental evaluation

Experiments were performed to assess PILM for visualisation and extraction of flow characteristics.

2.2.1. Visualisation of static objects

Two static objects of identical dimension were placed in a phantom as shown in Figure 4. Sensors from a 16 electrode EIT system were connected to the phantom. Measurements were performed using conventional adjacent sensing strategy. Conductivity reconstruction was performed for adjacent measurement as well as PILM. Measurements necessary for PILM were extracted from the set of data collected for adjacent measurement.

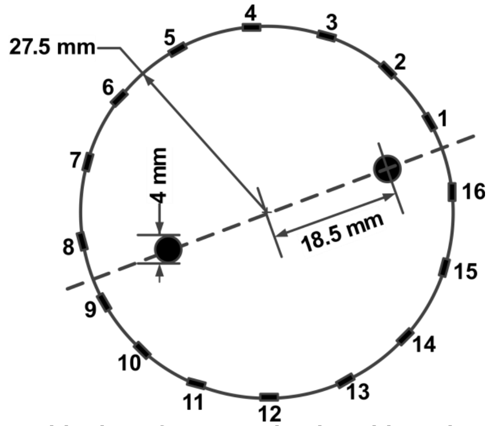

Figure 4: positioning of non-conductive objects in a phantom

2.2.2. Concentration and velocity profile mapping for 2 phase flow

Further experiments were conducted using the air-water 2-phase upward flow in vertical pipeline with inner diameter of 50mm at the University of Leeds. Slug flow regime was tested with water and air flowing at 27 rpm and 70 litre/min, respectively. A fast 16 electrode EIT system (FICA) was used to collect data at a speed of 1000dfps. Data for PILM was extracted from the full set of measured data and velocity and concentration profiles were generated in both cases.

3 RESULTS

3.1. Visualisation of static objects

Figure 5 demonstrates the visualisation results of two non-conductive static objects in a phantom, using conventional conductivity tomogram and PILM. Since PILM is only concerned with the central area of the grid, it is more meaningful to compare the central area of the tomograms. Only the central four rows of the full tomogram shown in Figure 5 (a) are shown in Figure 5 (b). The partial tomogram resulting from PILM is capable of visually identify the objects as shown in Figure 5 (c). Masked tomogram (Figure 5 (b)) and partial tomogram from PILM (Figure 5 (c)) are not visually identical as the range of measurement is different between them.

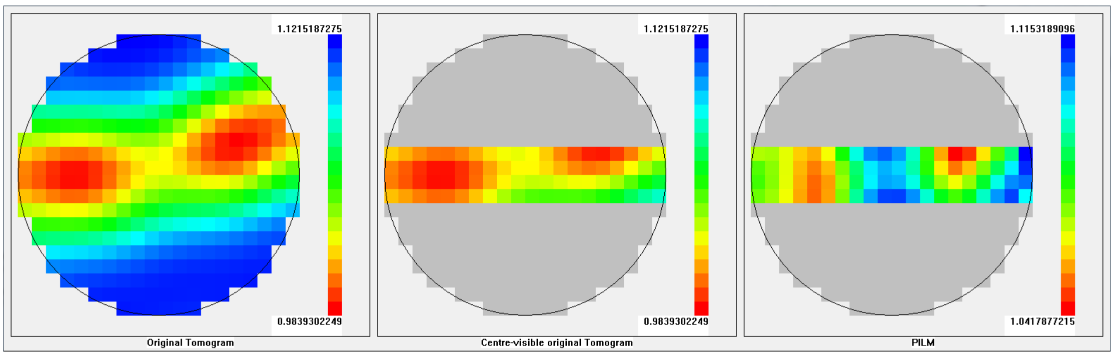

(a) (b) (c)

Figure 5: Conventional tomogram and PILM-generated tomogram of 2 static objects in a phantom: (a) original tomogram, (b) centre-visible original tomogram, (c) tomogram from PILM

3.2. Concentration and velocity profile mapping for 2 phase flow

Stacked images for two-phase slug flow described in 2.2.2 were reconstructed from full measurement and PILM measurement as shown in Figure 6. Average of the central four rows of the tomograms was used in the stacked images. PILM was able to produce comparable visualisation with respect to full measurement.

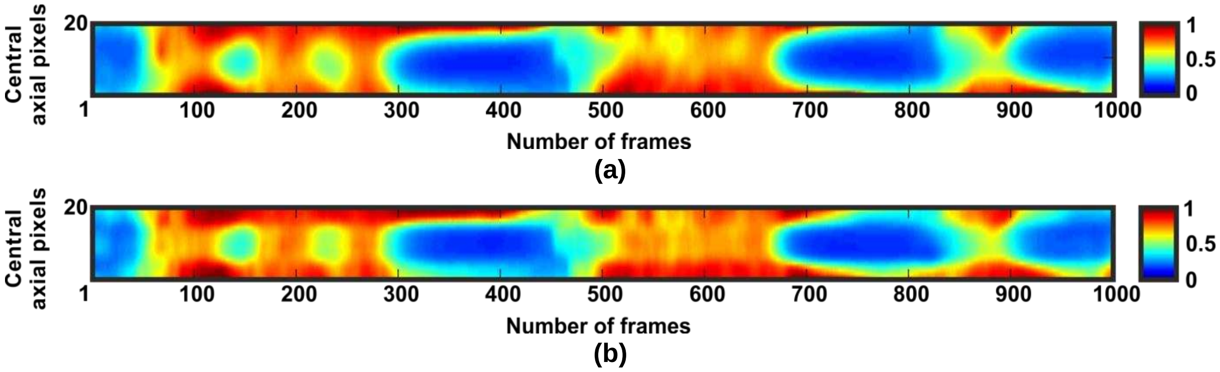

Figure 6: Stacked image of two phase flow: (a) from full measurement, (b) from PILM

The concentration and velocity profiles were obtained from full measurement as well as PILM for air-water upward two-phase flow in vertical pipeline are illustrated in Figure 7 (a) and (b) respectively. The profiles were calculated from the mean value of reconstructed tomograms. Similar characteristics are demonstrated by the profiles obtained from both strategies. The difference between them is more pronounced towards the boundary than the centre of the pipe. This difference is highlighted by Figure 7 (c) and (d) which shows the percentage of error between the two methods with respect to the full measurement.

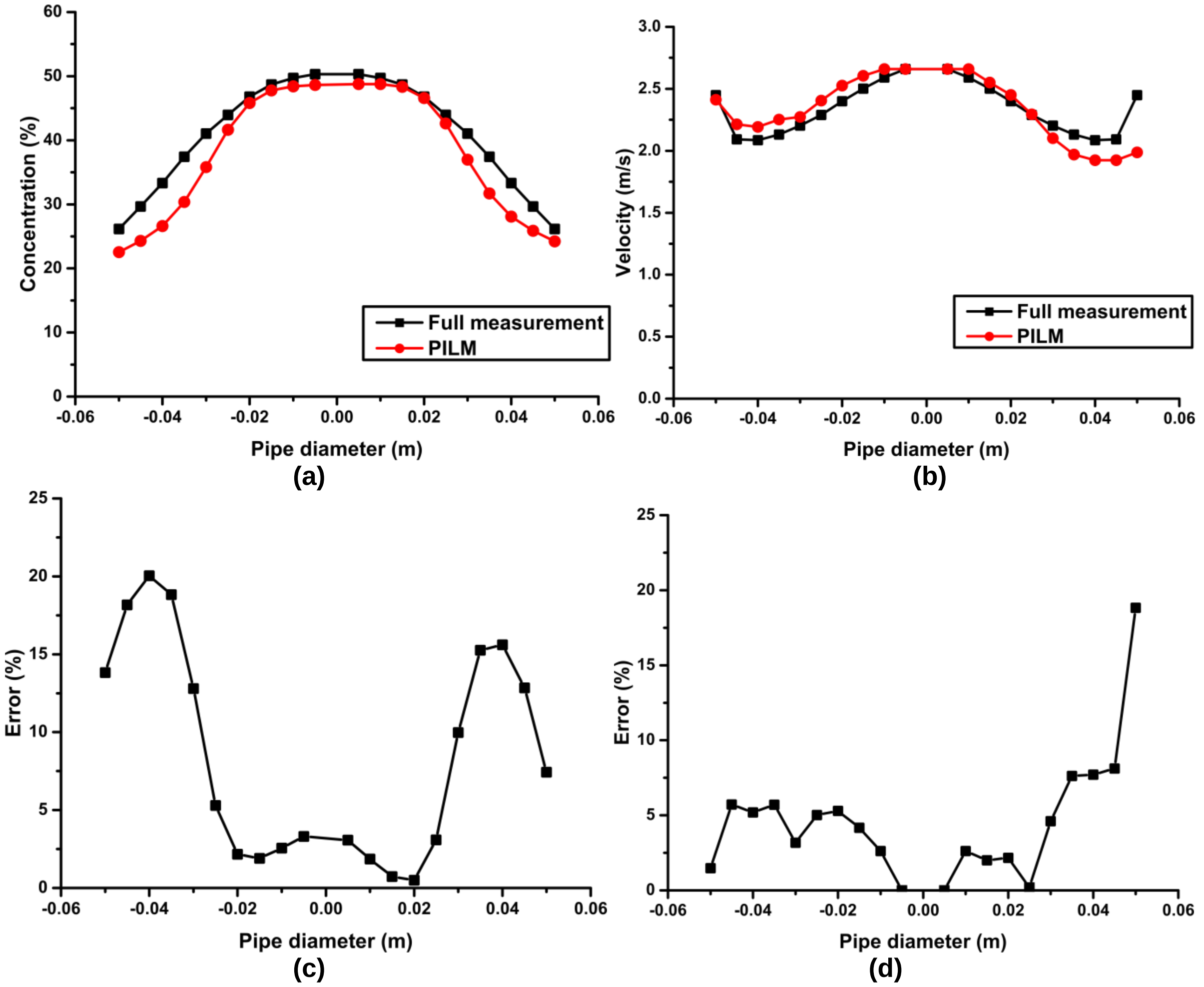

Figure 7: (a) Concentration profile, (b) Velocity Profile, (c) Percentage error in concentration profile (d) Percentage error in velocity profile

4 CONCLUSIONS

A new approach that partially images multiphase flow by limiting the number of measurements based on conventional 16 electrodes EIT was investigated to visualise non-conductive objects in a phantom and meter air-water two-phase upward flow in vertical pipeline. The study demonstrated the performance of the proposed approach. From visualisation point of view, PILM is able to clearly illustrate the size and position of the objects. From measurement perspective, it is also capable of producing comparable results in terms of concentration and velocity profiles, although there are some small errors at boundary area, which may result from the weaker accumulation of electrical filed at boundary area by PILM, compared to the electrical field generated by conventional EIT system with 16-electrode configuration. Although the experiments were conducted on vertical pipeline flow, it is possible to adapt PILM to horizontal pipeline flow as well since tomograms of steady-state horizontal pipeline flow are symmetrical to its vertical diameter.

Since PILM requires considerably lesser number of measurements, it is reasonable to anticipate that PILM could outperform conventional EIT systems in terms of measurement speed. The speed offered by PILM could result in reduction of discrimination error, and therefore significant improvement in velocity calculation. However, there are still several issues that will be the subject of future investigations. The profiles suffer from error closer to the boundary of the pipeline. One probable cause for this error might be weak electrical field produced by less injection and measurement pairs. It can be reduced by reasonably increasing the number of injection and/or measurement pairs. This issue merits further investigation and analysis. Another aspect to be investigated is the feasibility of proposed method in horizontal and inclined pipeline flow where injection and measurement pairs must be chosen carefully.

ACKNOWLEDGEMENT

This research was supported by European Association of National Metrology Institutes, project ENG58-REG2, Multiphase flow metrology in oil and gas production. The EMRP is jointly funded by the EMRP participating countries within EURAMET and the European Union.

REFERENCES

BARBER, D. C. and BROWN, B. H., (1984), Applied potential tomography, Institute of Physics

BECK, M.S. and PLASKOWSKI, A., (1987), Cross Correlation Flowmeters -Their Design and Application, CRC Press

BRECKON, W R and PIDCOCK, M K, (1987), Mathematical aspects of impedance imaging, Clinical Physics and Physiological Measurement, 8 351-362

DA TORRE PINHEIRO, P.A., (1994), Investigation of Forward Problem Solvers and Data Collection Methods in Electrical Impedance Tomography, UMIST

HUA, P., WEBSTER, J.G. and TOMPKINS, W.J., (1987), Effect of the measurement method on noise handling and image quality of EIT imaging, Proc. Annu. Int. Conf. Engng Med. and Biol. Soc., 9 1429-1430

KOTRE, C J, (1994a), EIT image reconstruction using sensitivity weighted filtered backprojection, Physiological Measurement, 15 A125

KOTRE, C J, (1994b), EIT image reconstruction using sensitivity weighted filtered backprojection, Physiological Measurement, 15 A125-A136

SYSTEMS, INDUSTRIAL TOMOGRAPHY, (2009), ITS System 2000 Version 7.0 p2+ Electrical Resistance Tomography System - User's Manual

WANG, M., (2002), Inverse solutions for electrical impedance tomography based on conjugate gradients methods, Measurement Science and Technology, 13 101